Available online at www.eccomasproceedia.org
Eccomas Proceedia COMPDYN (2025) 264-275

ECCOMAS
Proceedia

COMPDYN 2025
10th ECCOMAS Thematic Conference on
Computational Methods in Structural Dynamics and Earthquake Engineering
M. Papadrakakis, M. Fragiadakis (eds.)
Rhodes Island, Greece, 15-18 June 2025

COMPARATIVE STUDY OF SOLID AND SHELL ELEMENTS IN THE NUMERICAL MODELLING OF HERITAGE STRUCTURES

Isabel González-de-León[1], Maria Victoria Requena-Garcia-Cruz[2], Emilio Romero-Sánchez[2] and Antonio Morales-Esteban[3]

[1] Department of Building Structures and Geotechnical Engineering, University of Seville, Spain
igonzalez4@us.es

[2] Department of Mechanical Engineering and Industrial Design, University of Cadiz, Spain
{mariavictoria.requena, emilio.romero}@uca.es

[3] Instituto Universitario de Ciencias de la Construcción. University of Seville. Spain
ame@us.es

Abstract

Numerical modelling of heritage structures presents unique challenges due to their complex geometry, material heterogeneity and intricate structural behaviour. This study compares the performance of solid and shell elements in simulating the seismic response of historical masonry structures and aims to identify the most effective modelling approach for accurately capturing both the structural and dynamic characteristics of these complex architectural systems. An arcade of the Mosque-Cathedral of Cordoba, where one dimension predominates over the other two, has been used as a case study. Three different models have been developed and discretised in the STKO framework using solid, solid-shell-beam and solid-shell elements. Modal analyses have been carried out using the open source software OpenSees. The results reflect a small disparity in the first modes of vibration exhibited by the solid element reference model and the two shell element models, mainly caused by the different boundary conditions. However, the computational cost of the shell models is much lower, so the use of this finite element may be of interest when analysing large-scale heritage buildings. This study highlights the critical importance of selecting an appropriate modelling strategy depending on the specific requirements of the analysis, the characteristics of the structure and the desired level of detail. This knowledge is valuable for engineers and conservators involved in the seismic assessment and conservation of historic architectural heritage.

Keywords: Heritage structures, Seismic response, Numerical modelling, Shell element, Solid element, OpenSees.

Peer-review under responsibility of the organizing committee of COMPDYN 2025.
doi: 10.7712/120125.12407.24958

1 INTRODUCTION

The conservation of built heritage has become of paramount importance for society, as heritage buildings are a sign of the culture of a region, e.g., they are a living proof of the technical achievements of that society at a certain time [1], and are inseparable from its identity. Therefore, there is a growing interest in improving the methodology of assessment and increasing the knowledge on the construction methods to ensure their conservation [2–8].

Structural analyses are essential to assess the current state of historic buildings [9]. From structural analyses it is not only possible to determine the safety level of the building, but also to better understand its structural behaviour and to propose effective reinforcement measures. Structural analyses allow the simulation of other catastrophes to which the building may be subjected, such as an earthquake. It should be remembered that earthquakes are the natural phenomenon with the most destructive economic, socio-cultural and demographic consequences. 2009 L'Aquila, 2011 Lorca and 2017 La Puebla earthquakes are just three recent examples that highlighted the weakness of our heritage. However, studying the structural behaviour of heritage buildings under seismic loads is a complex task, as they present aseismic designs, undergo several transformations over the years and it is very difficult to characterise the mechanical properties of the materials used in their structural elements [2]. For this reason, sectors or case studies are often studied in detail and then extrapolated to other sectors or similar buildings [10].

Although there are several modelling strategies to study the seismic behaviour of a masonry heritage building [11], the Finite Element (FE) method is the most widely used due to its accuracy. Numerical models in the FE method can follow two different modelling approaches: the micro-numerical approach, where the bricks and mortars are explicitly defined, and the macro-numerical approach, where the masonry wall is defined as a continuum deformable body, and it discretised into beam, shell or solid elements. Of these, solid elements are the most used in the evaluation of historic buildings, as they accurately capture the stress-strain behaviour of materials. However, they require significant computational effort and may not be efficient when analysing large-scale sectors. Macro-numerical approaches usually make use of nonlinear continuum constitutive law models to represent the global mechanical response of the masonry [12]. Due to the level of protection of heritage buildings, these laws models are usually calibrated using experimental data from non-destructive tests (NDT) performed on site or from the literature. The overall numerical model is usually validated by comparing its modal response with experimental data obtained from an operational modal analysis (OMA) [13–17].

In this context, this study investigates the comparative performance of solid and shell FE in simulating the modal response of historical masonry structures and aims to identify the most effective modelling approach for accurately capturing both the structural and dynamic characteristics of these complex architectural systems. To do so, an arcade of the Great Mosque-Cathedral of Cordoba from the Abd al- Rahman I sector, which dated from the 8th century, have been considered as case study. The Great Mosque-Cathedral of Cordoba is one of the most exceptional monuments in the world, declared by the UNESCO a 'World Heritage Site' in 1984 and a 'Site of Outstanding Universal Value' (the highest recognition) in 2014 [18]. The models have been developed in the STKO software, while the modal analyses have been performed in the OpenSees framework [19]. The geometric and material characteristics have been taken from a previous numerical study focused on the seismic behaviour of the whole Abd al-Rahman I sector carried out by the authors and available in [17,20].

This paper is divided as follows. In §2, a brief historical introduction of the case study is presented, focusing on the research performed up to date, as well as the geometry and construction characteristics. In §2, the numerical models (i.e., the solid-FE model based on the one developed in [17] and the shell-FE models developed on purpose for this study) are described. In §4, the results from the analyses on solid-FE and shell-FE models are shown. The discussion of the results is presented in §5. Finally, conclusions and future developments are summarised in §6.

This study emphasizes the importance of selecting an appropriate modelling strategy based on the specific requirements of the analysis, the structure's characteristics and the desired level of detail. These insights are valuable for engineers and conservators involved in the seismic assessment and preservation of historical architectural heritage.

2 CASE STUDY: THE ARCADES OF THE GREAT MOSQUE-CATHEDRAL OF CORDOBA

The Great Mosque-Cathedral of Cordoba is one of the most remarkable buildings of the Hispano-Muslim art [18]. It has north-south orientation and its overall measures are 130 m-length and 50 m-width. Its construction spans several centuries (from the 8th to the 16th century), as it has undergone several extensions and adaptations, such as the transition from an Islamic to a Christian temple. The building can be sectorised into 8 sectors according to the data of extensions undergone.

The primitive mosque, i.e., the Abd al-Rahman I sector, was started in 785 and finished in 787 [21]. The overall dimensions of this sector are 20 m long and 90 m wide, and it is defined by eleven parallel naves, separated by arcades with double arches unheard of in Islamic religious architecture [18] with widths ranging from 6.83 m to 7.83 m. Figure 1 shows the plan of the sector with the nomenclature for the naves established by the maintenance plan. The arcades are composed by an upper semicircular arch and a lower horseshoe-shaped arch. The construction of the Abd al-Rahman I sector was carried out by reusing materials from surrounding dismantled buildings. The columns (bases, shafts, capitals and cymatiums) are made of marble, granite and limestone from the Roman Empire and the Visigothic Kingdom [22]. The walls are made of brick and limestone masonry. The double arches are made of voussoir stone interspersed with bricks, originating to the well-known bi-chromatism. The roofs were made of timber with rafters spaced 0.8-0.9 m apart. At the beginning of the 20th century, the wooden structure of all the naves, except nave N14, was replaced by steel trusses. Finally, the walls of the perimeter were made of limestone masonry.

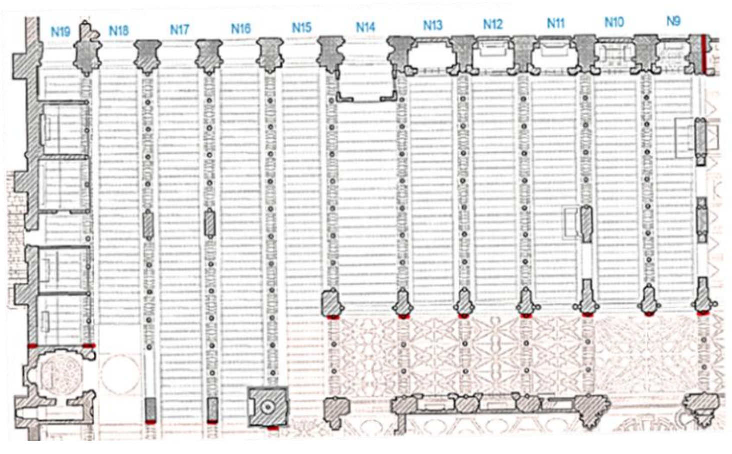

Figure 1: Plan of the Abd al-Rahman I sector adapted from [23]. Contact with the adjacent sectors marked in red and arcade studied in this paper highlighted.

The Mosque-Cathedral of Cordoba is in a region affected by the convergence between the Eurasian and African tectonic plates that currently has a moderate level of seismicity, although there is record of large earthquakes in the past [24]. In light of this, the authors have already carried out a comprehensive study of the structural and seismic behaviour of the Abd al-Rahman I sector, which includes an exhaustive visual inspection of the sector, the review of the literature, the performance of several NDT tests to identify the materials characteristics, including an OMA analysis to identify the dynamic behaviour of the sector, the development of a detailed finite element model, the proposal of the mechanical parameters of each material based on numerical calibrations and the analysis of the sector under different seismic scenarios. Results are detailed in [17,20].

This study focuses on arcade N16-N17 (see Figure 1). Figure 2 shows an overview of the case study, pointing out the thicknesses observed in the different parts that compose it. The massive external and internal walls are of limestone masonry. For the sake of simplicity, in this study the rest of the arcade is assumed to be of the same brick masonry, while all the columns are assumed to be of granite. Table 1 shows the material properties of interest for this study and based on those published in [17], i.e., the density ρ, Young's modulus E and Poisson's coefficient v.

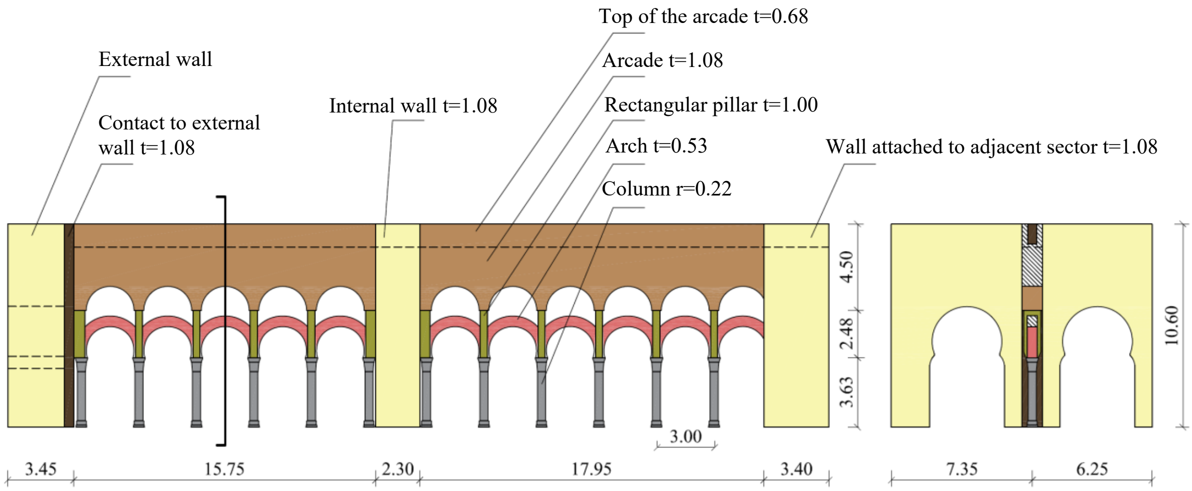

Figure 2: Frontal view and section of the arcade case of study (annotations in meters).

Material	ρ (T/m^3)	E (GPa)	v
Limestone masonry	1.8	2.5	0.3
Brick masonry	1.8	2.0	0.2
Granite	2.8	29.0	0.25

Table 1: Key material properties considered in this study and based on [17].

3 NUMERICAL MODELLING

This study aims to compare the modal behaviour performed by solid-FE and shell-FE macro-numerical models. A total of three 3D numerical models of the arcade N16-N17, have been developed: (1) a complete solid-FE model which is the benchmark, (2) a shell-FE model with beam-FE columns, and (3) a shell-FE model with solid-FE columns. The study was carried out in the OpenSees framework [19], which is an open source software specific for earthquake-engineering analyses. The FE meshing was developed in the STKO software [25], a pre- and post-processor for OpenSees. The models have been calculated with the parallel option available in OpenSees and using multiprocessors. As only modal analyses have been run, the models have been split into a single partition. The analyses have been carried out on a computer with an Intel(R) Core(TM) i9 14900HX processor.

3.1 Solid-FE model: benchmark FE model

The benchmark FE model of the arcade N16-N17 was developed based on the solid-FE model described in [17]. A realistic 3D geometric model was previously created in Rhinoceros [26], and then imported to the STKO software, where it was discretised using the solid element 'FourNodeTetrahedron' from the OpenSees library. The mesh size was set to 0.5 m long elements (see Figure 3(a)).

As for the boundary conditions, fixed constraints were introduced at the base of the structure (external and internal walls and column bases). All the elements of the numerical model were considered as perfectly connected. For this purpose, the different volumes were merged into a single volume. The adjacent sector was simulated as a 2D surface attached to the arcade. All degrees of freedom of the surface were restricted, acting as a reaction wall. The connection of the arcade to the wall of the adjacent sector was simulated modelling a 'node-to-node' interaction and using the 'ZeroLengthContact3D' element available in [19]. As in similar works [27], the contact forces were defined to follow the classical Mohr-Coulomb criterion: $T = \mu \cdot N + c$, where T is the tangential force and N is the normal force across the interface, μ is the friction coefficient and c is the total cohesion. Adopting the assumptions defined in [17], i.e., regular masonry pattern and good quality of bricks and mortar, the values of the parameters were $\mu = 0.5$ and c = 100 kPa [27]. In addition, to proper defined the constitutive Mohr-Coulomb law applied at the 'ZeroLengthContact3D' element, values for the joint normal stiffness and the joint shear stiffness are needed [27]. The values of stiffness in the normal (K_n) and the shear (K_s) direction were 2e9 and 6e8 kPa/m, respectively [17].

Although this study is based on linear analyses, the material models introduced in the solid-FE model were equivalent to those used in [17]. Thus, the nonlinear behaviour of the materials involved in the structure, i.e., limestone masonry, brick masonry and granite, was simulated using the damage-plasticity material constitutive law developed by Petracca et al. [28,29] for brick masonry walls and implemented in STKO and Opensees as 'DamageTC3D' (3D Tension-Compression Damage Model).

3.2 Shell-FE with beam-FE columns

A first shell-FE model of the arcade N16-N17 was developed based on a 2D geometric model. The arcade (brick masonry over the arches, arches, and rectangular pillars) was modelled as 2D surfaces. The external and internal walls were modelled as 3D elements due to their massiveness compared to the arcade. The columns were modelled as lineal elements.

In the STKO framework, the arcade was discretised using the 3-node general purpose thick shell element 'ASDShellT3'. Triangular elements were chosen over quadrangular elements due to the geometry of the arches. As in the benchmark model, the walls were discretised using 'FourNodeTetrahedron' solid elements. Finally, columns were modelled using 'ForceBeamColumn' elements and assigned a circular section of radius 0.22 m using the 'FiberSection' option available in [19]. The section of the column was discretised into 0.1 m long triangular elements in order to preserve the circular geometry. For the rest of model, the mesh size was set to 0.5 m long elements (see Figure 3(b)).

As in the benchmark model, fixed constraints were introduced at the base of the structure (external and internal walls and columns). To ensure that the structure was perfectly connected, all the surfaces (shell) that constituted the arcade were fused, and 'node-to-node' interactions were introduced to connect it to walls (solid) and columns (beam). The interaction between the arcade and the walls was defined with the master nodes being the edge of the arcade and the slave nodes being the wall contact surfaces, and applying a 'BeamSolidCoupling' condition. The interaction of the arcade and the columns was defined with the master node being the centre node of the rectangular pillar and the slave node being the top node of the column, and applying a 'RigidLink' condition. Finally, the 'ZeroLengthContact3D' element was used to connect the arcade to the adjacent sector, introducing the same contact forces as in the solid-FE model.

Regarding the material properties, the 'DamageTC3D' model was used to define the nonlinear behaviour of the limestone masonry and brick masonry. Since this model material cannot be assigned to 'ForceBeamColumn' elements, the 'ASDConcrete1D' physical property model was used to simulate the mechanical behaviour of the granite material together with an 'AutoEdgeMass' condition assigned to columns to introduce the corresponding mass.

3.3 Shell-FE with solid-FE columns

The 'ForceBeamColumn' elements are lineal elements where boundaries conditions are applied to the central fibre, so the benchmark model is much rigid than the shell-FE model explained in §3.2. In light of this, a second shell-FE model was developed, the same as the previous one but replacing the beam-FE columns with solid-FE columns. Since the column bases in the benchmark model were square, in this shell-FE model columns have square-sections of area equal to the area of the circular-section columns, i.e., 0.39 m on a side. As for the boundary conditions, the bottom face of the columns was completely fixed, while the top face was connected to the arcade through 'node-to-node' interactions. 'BeamSolidCoupling' conditions were assigned to these interactions, with the master nodes being the edge of the rectangular pillars in contact with the columns. Finally, as in the benchmark model, the behaviour of the granite material was introduced using the 'DamageTC3D' model and the mass condition was removed.

4 ANALYSES AND RESULTS

This section presents the differences in geometry, computational efficiency and modal analysis results between the three models: the solid-FE model (the most accurate and therefore considered as the reference model), the shell-FE model with beam-FE columns (hereafter shell$_{BC}$-FE), and the shell-FE model with solid-FE columns (hereafter shell$_{SC}$-FE). Results are discussed in detail in the following section.

4.1 Modelling comparison: volumes and masses

Figure 3 shows the (a) solid-FE and (b) shell$_{BC}$-FE macro-numerical models, highlighting the boundary conditions. Table 2 reports the approximate volumes of the different parts that constituted the solid-FE and shell-FE models (see Figure 2). Table 3 summarised the total mass and torsional masses given by OpenSees after conducting the modal analyses for the solid-FE, shell$_{BC}$-FE and shell$_{SC}$-FE models.

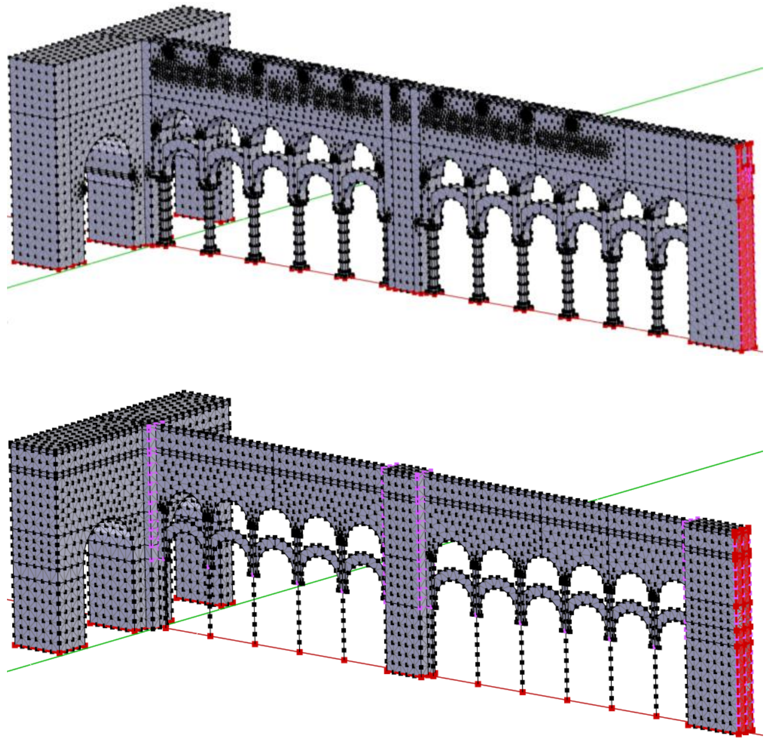

Figure 3: (a) Solid-FE and (b) shell-FE with beam-FE columns, i.e., $shell_{BC}$-FE, models of the case study.

Part	Material	Volume (m3)	
		Solid-FE	Shell-FE
External wall	Limestone masonry	303.13	294.85
Internal wall		26.17	26.33
Wall attached to adjacent sector		37.92	38.92
Contact to external wall	Brick masonry	6.31	5.15
Top of the arcade (water evacuation)		26.81	27.50
Arcade		90.75	91.01
Rectangular pillars (n=12)		11.35	12.60
Arches (n=11)		11.10	10.73
Columns (n=12)	Granite	6.97	6.61

Table 2: Approximate volumes in solid-FE and shell-FE models.

	Solid-FE	$Shell_{BC}$-FE	Solid-FE / $Shell_{BC}$-FE	$Shell_{SC}$-FE	Solid-FE / $Shell_{SC}$-FE
Mass (t)	942.98	933.23	1.01	933.95	1.01
Torsional mass X (kNm)	16944.1	16560.5	1.02	16578.2	1.02
Torsional mass Y (kNm)	184469	184606	1.00	184761	1.00
Torsional mass Z (kNm)	185890	185906	1.00	186043	1.00

Table 3: Masses obtained from modal analyses.

4.2 Computational efficiency: meshing time

Table 4 reports the number of nodes and elements once the models were discretised. The time spent on the mesh generation is also given.

	Solid-FE	Shell$_{BC}$-FE	Solid-FE / Shell$_{BC}$-FE	Shell$_{SC}$-FE	Solid-FE / Shell$_{SC}$-FE
Number of nodes	23,446	6,690	3.50	6,995	3.35
Number of elements	129,942	34,900	3.72	36,995	3.51
Meshing time (s)	11.196	1.123	9.97	0.115	97.36

Table 4: Computational efficiency of the models.

4.3 Dynamic behaviour: frequencies and first modes of vibration

Table 5 shows the frequencies obtained for the first six modes from modal analyses, while Table 6 shows the corresponding the modal participation mass ratios in the principal directions, with X and Y being the in-plane and out-of-plane and directions, respectively.

Mode	Solid-FE Freq (Hz)	Shell$_{BC}$-FE Freq (Hz)	Solid-FE / Shell$_{BC}$-FE	Shell$_{SC}$-FE Freq (Hz)	Solid-FE / Shell$_{SC}$-FE
1	1.56	1.40	1.12	1.69	0.92
2	2.72	2.52	1.08	2.81	0.97
3	4.49	4.08	1.10	4.32	1.04
4	4.83	5.02	0.96	5.13	0.94
5	5.48	5.41	1.01	5.47	1.00
6	5.83	5.79	1.01	5.83	1.00

Table 5: Frequencies for the first six modes.

Mode	Solid-FE		Shell$_{BC}$-FE		Shell$_{SC}$-FE	
	Mass X (%)	Mass Y (%)	Mass X (%)	Mass Y (%)	Mass X (%)	Mass Y (%)
1	-	24.73	-	24.09	-	23.27
2	0.01	0.17	-	0.13	-	0.10
3	1.32	13.08	-	8.95	0.01	9.79
4	66.63	0.59	67.09	0.29	65.57	0.48
5	0.11	38.02	0.39	36.30	0.75	38.39
6	0.26	0.09	0.23	4.85	0.35	2.02

Table 6: Modal participation mass ratios in X and Y directions for the first five modes.

5 DISCUSSION

Table 3 shows that both shell-FE models accurately reproduce the total mass and torsional masses exhibited by the solid-FE model. The differences are attributed to the simplified geometry developed for the shell-FE models. As can be seen in Figure 2 and checked in Table 2, the external wall and columns are much more detailed in the reference model and have a slightly larger volume. Therefore, the masses computed for solid-FE model are higher than those of the shell-FE models.

In terms of computational efficiency (Table 4), both shell-FE models have one third of the nodes used in the solid-FE model. It is worth noting that the shell$_{BC}$-FE model has a mesh with fewer elements but uses practically the same number of nodes as the shell$_{SC}$-FE model. The shell$_{SC}$-FE model proved to be the most computationally efficient. The time taken to discretise this model was 0.115 s, i.e., almost 100 times less than the solid-FE model and 10 times less than the shell$_{BC}$-FE model. The simplification of the geometry partly explains the lower number of elements in the discretised shell-FE models. However, the lower number of elements and, consequently, the reduction of meshing time by about 10 and 100 times, is mainly due to the use of shell and beam elements, which are known to be more computationally efficient.

As Table 5 shows, all FE models exhibit similar modes of vibration. The $shell_{BC}$-FE model tends to underestimate the frequency values exhibited by the benchmark model, i.e., the solid-FE model, especially in the first modes. Since the masses are practically equal, this disparity is mainly due to the different boundary conditions: as mentioned above, the bottom surface of the square-section column base is fixed to the ground in the benchmark model, i.e., four nodes are constrained, while in $shell_{BC}$-FE model the column is constrained only at the central point. The $shell_{SC}$-FE model tends to overestimate the frequency values exhibited by the benchmark model in the first modes, but in general lines, the prediction is more accurate than those given by $shell_{BC}$-FE model.

Finally, the results reported in Table 6 reveal that most of the modes have a noticeable rotational involvement because the adjacent sector was defined as perfectly fixed and the diaphragm effect caused by the roof and timber was not modelled. As shown, both shell-FE models exhibit modal participation mass ratios in X and Y directions similar to those obtained from the solid-FE model for the first six modes.

It should be noted that the differences between the frequency values and mass participation ratios reported in this study and those published in [17] are explained by the fact that this model is limited to one arcade, only three materials were introduced, and the effect of the roof and timber was not taken into account.

Based on the results, it can be concluded that the shell-FE models can be an appropriate modelling approach in the case of large-scale heritage building, where the computational efficiency is of paramount importance. The use of shell elements, either partially, as in this study, or fully, if the model has a much lower dimension than the other two dimensions, reduces the meshing time considerably. However, it is worth mentioning that solid elements are widely used in the assessment of heritage structures, as they provide a complete stress-strain behaviour of elements and materials. Therefore, further research on the performance of shell-FE models in different seismic analyses compared to solid-FE models is needed to fully adopt shell-FE elements in heritage seismic vulnerability assessment.

6 CONCLUSIONS

Numerical modelling of heritage structures poses significant challenges due to their complex geometry, heterogeneity of materials and intricate structural behaviour. Due to their accuracy in reproducing stress-strain behaviour, heritage structures are usually evaluated by solid-FE numerical modelling. However, even in cases where only one sector of the entire heritage building is studied, solid-FE models are often time-consuming, both in terms of meshing and analysis.

In order to identify the most effective modelling approach to accurately capture the structural and dynamic characteristics of these complex architectural systems, the present study has compared the performance of solid and shell elements in simulating the modal response of historic masonry structures and their targets. An arcade of the Great Mosque-Cathedral of Cordoba, in which one dimension predominates over the other two, was used as a case study. Three different models were developed and discretised in the STKO framework: (1) a fully solid-FE model (considered the benchmark), (2) a shell-FE model in combination with solid and beam elements and (3) a shell-FE model with punctual solid elements. Modal analyses were carried out using the open source software OpenSees. The results reflect that the small discrepancies between models are due to the boundary and connection conditions between structural parts discretised with different elements. However, this disparity is compensated by the significant reduction in time when discretising with shell elements (up to 100 times shorter), due to the efficiency of these elements and the simplification of the geometry involved in their use. This knowledge can be valuable for engineers and conservators involved in seismic assessment and conservation of historic architectural heritage, who may not have access to powerful processors.

The present study highlights the critical importance of selecting an appropriate modelling strategy depending on the specific requirements of the analysis, the characteristics of the structure and the desired level of detail. However, it should be noted that the conclusions presented herein are based on modal results. To really consider shell-FE models as a reasonable alternative to solid-FE models, it is necessary to study their performance under different seismic analyses.

ACKNOWLEDGEMENTS

This manuscript is part of the R+D+i project ‘Metodología avanzada para la evaluación de la seguridad estructural y sísmica de edificios patrimoniales’, grant ‘Proyecto PID2023-150771OB-I00’ funded by ‘MCIN 10.13039/501100011033’ and by the ‘European Union’. The authors would like to thank the Cabildo Catedralicio of Cordoba for their support. Especially, the authors want to thank the architect Gabriel Rebollo Puig for his outstanding to help. The funding provided by the *Instituto Universitario de Arquitectura y Ciencias de la Construcción* is also acknowledged.

REFERENCES

[1] ICOMOS - International Council of Monuments and Sites. International Charter for the conservation and restoration of monuments and sites (The Venice Charter), Venice: 1964.

[2] Lagomarsino S, Cattari S. PERPETUATE guidelines for seismic performance-based assessment of cultural heritage masonry structures. Bulletin of Earthquake Engineering 2015;13:13–47. https://doi.org/10.1007/s10518-014-9674-1.

[3] MICRO-PAR project 2013. https://futur.upc.edu/11212603 (accessed January 19, 2024).

[4] MULTIMAS project 2018. https://futur.upc.edu/17980111 (accessed January 19, 2024).

[5] Hyperion Project 2019. https://www.hyperion-project.eu/ (accessed January 11, 2024).

[6] STAND4Heritage project 2020. https://stand4heritage.org/ (accessed January 11, 2024).

[7] HOLAHERIS project 2020. https://site.unibo.it/holaheris/en (accessed January 11, 2024).

[8] SEVERUS project 2022. https://futur.upc.edu/24476359 (accessed January 19, 2024).

[9] Roca P, Cervera M, Gariup G, Pela’ L. Structural Analysis of Masonry Historical Constructions. Classical and Advanced Approaches. Archives of Computational Methods in Engineering 2010;17:299–325. https://doi.org/10.1007/s11831-010-9046-1.

[10] Bento R. Analysis Case Studies in Evaluation, Rehabilitation and Reconstruction of the Built Heritage. European Conference on Earthquake Engineering and Seismology, Springer; 2022, p. 245–60. https://doi.org/10.1007/978-3-031-15104-0_15.

[11] Cattari S, Calderoni B, Caliò I, Camata G, de Miranda S, Magenes G, et al. Nonlinear modeling of the seismic response of masonry structures: critical review and open issues towards engineering practice. Bulletin of Earthquake Engineering 2022;20:1939–97. https://doi.org/10.1007/S10518-021-01263-1.

[12] D'Altri AM, Sarhosis V, Milani G, Rots J, Cattari S, Lagomarsino S, et al. Modeling Strategies for the Computational Analysis of Unreinforced Masonry Structures: Review and Classification. Archives of Computational Methods in Engineering 2020;27:1153–85. https://doi.org/10.1007/s11831-019-09351-x.

[13] Kita A, Cavalagli N, Venanzi I, Ubertini F. A new method for earthquake-induced damage identification in historic masonry towers combining OMA and IDA. Bulletin of Earthquake Engineering 2021;19:5307–37. https://doi.org/10.1007/S10518-021-01167-0.

[14] Ponte M, Bento R, Vaz SD. A Multi-Disciplinary Approach to the Seismic Assessment of the National Palace of Sintra. International Journal of Architectural Heritage 2021;15:757–78. https://doi.org/10.1080/15583058.2019.1648587.

[15] Ozcelik O, Misir IS, Yucel U, Durmazgezer E, Yucel G, Amaddeo C. Model updating of Masonry courtyard walls of the historical Isabey mosque using ambient vibration measurements. Journal of Civil Structural Health Monitoring 2022 2022:1–16. https://doi.org/10.1007/S13349-022-00610-3.

[16] Romero-Sánchez E, Morales-Esteban A, Bento R, Navarro-Casas J. Numerical modelling for the seismic assessment of complex masonry heritage buildings: the case study of the Giralda tower. Bulletin of Earthquake Engineering 2023;21:4669–701. https://doi.org/10.1007/s10518-023-01714-x.

[17] Requena-Garcia-Cruz MV, Romero-Sánchez E, López-Piña MP, Morales-Esteban A. Preliminary structural and seismic performance assessment of the Mosque-Cathedral of Cordoba: The Abd al-Rahman I sector. Eng Struct 2023;291:116465. https://doi.org/10.1016/j.engstruct.2023.116465.

[18] Word Heritage Committee. United Nations Educational. Inscription: The Mosque of Cordoba (Spain) (08COM IXA). Convention concerning the protection of the world cultural and natural heritage, 1984.

[19] McKenna F, Fenves GL, Scott MH. OpenSees: Open system for earthquake engineering simulation. Pacific Earthquake Engineering Research Center. Berkeley, CA: University of California; 2000.

[20] Requena-Garcia-Cruz M, Romero-Sanchez E, Morales-Esteban A. Dynamic performance of the Mosque-Cathedral of Córdoba under different earthquake scenarios: the Abd al-Rahman I sector. Journal of Building Engineering 2023;79. https://doi.org/10.1016/j.jobe.2023.107853.

[21] Sánchez-Albornoz C. La España musulmana según los autores islamitas y cristianos medievales (in Spanish). Madrid: Espasa-Calpe; 1973.

[22] Hidalgo Fernández RE, Ortiz-Cordero R. The Mosque-Cathedral of Córdoba: Evidence of column organization during their first construction s. VIII A.D. J Cult Herit 2020;45:215–20. https://doi.org/10.1016/j.culher.2020.05.011.

[23] Almagro Gorbea A. Arquitectura Al-Andalus. Catálogo digital de arquitectura RABASF, 2022.

[24] Amaro-Mellado JL, Morales-Esteban A, Martínez-Álvarez F. Mapping of seismic parameters of the Iberian Peninsula by means of a geographic information system. Cent Eur J Oper Res 2017. https://doi.org/10.1007/s10100-017-0506-7.

[25] Petracca M, Candeloro F, Camata G. STKO user manual. ASDEA Software Technology. Pescara, Italy: 2017.

[26] Rhino - Rhinoceros 3D n.d. https://www.rhino3d.com/ (accessed November 10, 2022).

[27] Ferrante A, Loverdos D, Clementi F, Milani G, Formisano A, Lenci S, et al. Discontinuous approaches for nonlinear dynamic analyses of an ancient masonry tower. Eng Struct 2021;230:111626. https://doi.org/10.1016/j.engstruct.2020.111626.

[28] Petracca M, Pelà L, Rossi R, Zaghi S, Camata G, Spacone E. Micro-scale continuous and discrete numerical models for nonlinear analysis of masonry shear walls. Constr Build Mater 2017;149:296–314. https://doi.org/10.1016/j.conbuildmat.2017.05.130.

[29] Petracca M, Pelà L, Rossi R, Oller S, Camata G, Spacone E. Multiscale computational first order homogenization of thick shells for the analysis of out-of-plane loaded masonry walls. Comput Methods Appl Mech Eng 2017;315:273–301. https://doi.org/10.1016/j.cma.2016.10.046.